

Distribution Agreement

In presenting this thesis as a partial fulfillment of the requirements for an advanced degree from Emory University, I hereby grant to Emory University and its agents the non-exclusive license to archive, make accessible, and display my thesis in whole or in part in all forms of media, now or hereafter known, including display on the world wide web. I understand that I may select some access restrictions as part of the online submission of this thesis. I retain all ownership rights to the copyright of the thesis. I also retain the right to use in future works (such as articles or books) all or part of this thesis.

Cyen J. Peterkin

Date

A Bayesian Hierarchical Excess Mortality Model to Assess the Total Impact of COVID-19 on
Opioid Users

By

Cyen J. Peterkin

Master of Science in Public Health

Department of Biostatistics and Bioinformatics

Emily N. Peterson, Ph.D.

(Committee Chair)

Alex Edwards, Ph.D.

(Committee Member)

Lance A. Waller, Ph.D.

(Committee Member)

A Bayesian Hierarchical Excess Mortality Model to Assess the Total Impact of COVID-19 on
Opioid Users

By

Cyen J. Peterkin

B.S., North Carolina Agricultural and Technical State University, 2022

B.S., North Carolina Agricultural and Technical State University, 2022

Committee Chair: Emily N. Peterson, Ph.D.

An abstract of

A thesis submitted to the Faculty of the
Rollins School of Public Health of Emory University
in partial fulfillment of the requirements for the degree of
Master of Science in Public Health
in the Department of Biostatistics and Bioinformatics

2024

Abstract

A Bayesian Hierarchical Excess Mortality Model to Assess the Total Impact of COVID-19 on Opioid Users

By Cyen J. Peterkin

COVID-19 has a large scale negative impact on the health of opioid users. As such, monitoring small-area opioid mortality trends has significant implications to informing preventative resource allocation. The total impact of COVID-19 on opioid users is unknown due to a lack of comprehensive data on COVID-19 cases, inaccurate diagnostic coding, and lack of data coverage. To assess the impact of COVID-19 on small area opioid mortality, we developed a Bayesian hierarchical excess opioid mortality modeling approach. We incorporate spatio-temporal autocorrelation structures to allow for sharing of information across small areas and time. Excess mortality is defined as the difference between the observed trends after a crisis and the expected trends based on observed historical trends, which captures the total increase in observed mortality rates compared to what was expected prior to the crisis. We illustrate the application of our approach to assess excess opioid mortality risk estimates for 159 counties in GA. Utilizing our proposed approach will help to inform interventions in opioid related public health responses, policies, and resource allocation. Additionally, we provide a general framework to improve in the estimation and mapping of health indicators during crisis periods.

A Bayesian Hierarchical Excess Mortality Model to Assess the Total Impact of COVID-19 on
Opioid Users

By

Cyen J. Peterkin

B.S., North Carolina Agricultural and Technical State University, 2022

B.S., North Carolina Agricultural and Technical State University, 2022

Committee Chair: Emily N. Peterson, Ph.D.

A thesis submitted to the Faculty of the
Rollins School of Public Health of Emory University
in partial fulfillment of the requirements for the degree of
Master of Science in Public Health
in the Department of Biostatistics and Bioinformatics

2024

TABLE OF CONTENTS

LIST OF TABLES

LIST OF FIGURES

| | | |
|----------|---|-----------|
| 1 | Introduction | 1 |
| 2 | Methods | 3 |
| 2.1 | Data | 3 |
| 2.2 | Summary of model approach | 5 |
| 2.3 | Data model for observed opioid-mortality counts | 6 |
| 2.4 | Process model for unobserved latent opioid mortality log-relative-risks | 7 |
| 2.5 | Derivation of Excess mortality and associated uncertainties | 8 |
| 3 | Computation | 9 |
| 4 | Results | 9 |
| 4.1 | Global Parameter Estimates | 9 |
| 4.2 | Excess Across Georgia | 10 |
| 4.3 | Large County Population Cases | 11 |
| 4.4 | Moderate County Population Cases | 13 |
| 4.5 | Small County Population Cases | 14 |
| 5 | Discussion | 16 |
| | Bibliography | 18 |
| | Appendix A Graphical representation of the BHEOM model | 23 |
| | Appendix B Notation Table | 24 |

LIST OF TABLES

| | | |
|---|---|---|
| 1 | Global and hyper parameters included in the random effect terms of the (BHEOM) model. | 9 |
|---|---|---|

LIST OF FIGURES

| | | |
|---|--|---|
| 1 | Monthly observed totals of opioid-related deaths across 159 counties in Georgia between the years 2018-2022. The red line denotes the defined start date of the COVID-19 pandemic (Jan. 2020). X-axis lists units in months ranging from 0 to 60, 0= Jan 2018, and 60 = Dec 2022. Colors denote years. | 4 |
| 2 | Mapped crude rates of opioid mortality (per 100,000) by year in Georgia between years 2018-2022. Color denotes the death rate per 100,000 which varies between 0 and 80. | 5 |

| | | |
|-----|--|----|
| 3 | Monthly totals of predicted, observed, and excess opioid-related deaths across 159 counties in Georgia between the years 2018-2020. The black line denotes the defined start of the COVID-19 pandemic in the model. The X-axis lists units in months ranging from 0 to 36, 0 = Jan 2018, and 36 = Dec 2020. Line colors distinguish the data source, red = observed deaths, lime green = predicted deaths, and blue = excess deaths. | 10 |
| 4 | Mapped excess rates of opioid mortality (per 100,000) by year in Georgia between years 2018-2020. Colors distinguish the rates and the rates vary between 0 and 9. | 11 |
| 5 | Monthly predicted, observed, and excess (and associated 95% confidence intervals) rates of opioid mortality (per 100,000) across DeKalb, Fulton, and Gwinnett County. The black line denotes the defined start of the COVID-19 pandemic in the model. The X-axis lists units in months ranging from 0 to 36, 0 = Jan 2018, and 36 = Dec 2020. Line colors distinguish the data source, red = observed deaths, lime green = predicted deaths, and blue = excess deaths. | 12 |
| 6 | Monthly predicted, observed, and excess (and associated 95% confidence intervals) rates of opioid mortality (per 100,000) across Bartow, Cherokee, and Clayton County. The black line denotes the defined start of the COVID-19 pandemic in the model. The X-axis lists units in months ranging from 0 to 36, 0 = Jan 2018, and 36 = Dec 2020. Line colors distinguish the data source, red = observed death rates, lime green = predicted death rates, and blue = excess death rates. | 14 |
| 7 | Monthly predicted (and associated 95% confidence intervals), observed, and excess (and associated 95% confidence intervals) rates of opioid mortality (per 100,000) across Toombs, Meriwether, and Walker County. The black line denotes the defined start of the COVID-19 pandemic in the model. The X-axis lists units in months ranging from 0 to 36, 0 = Jan 2018, and 36 = Dec 2020. Line colors distinguish the data source, red = observed death rates, lime green = predicted death rates, and blue = excess death rates. | 16 |
| A.8 | Directed graphical representation of the BHEOM hierarchical model. Shaded rectangles denote observed data quantities, and circles denote latent variables (shaded circles for global hyper-parameters). Solid arrows denote stochastic dependency. Boxes group quantities by indices, i.e., (1) Bottom box contains observed population data, stratified by county-month for years 2018-2019, (2) Middle box contains estimated parameters stratified by county-month, for years 2018-2020, (3) Top box contains global parameters. Subscripts refer to county i , month m | 23 |

1. Introduction

The vulnerable population of opioid drug users is situated at the intersection of two global epidemics: the opioid epidemic and the COVID-19 pandemic. This has resulted in a notable increase in opioid mortality rates. Monitoring of small area geographical-temporal opioid mortality trends during a crisis period has large-scale implications to informing public health policy, resource allocation, and public health response strategies (Wakefield, J., 2007). However, the lack of real-time cause-specific mortality data and issues related to inaccurate accounting of COVID-19 cases have created barriers to conducting a comprehensive, accurate, and robust assessment of the total impact of COVID-19 on the population of opioid users.

In March 2020, the World Health Organization declared COVID-19 a global pandemic, prompting the United States to implement a series of lockdowns to curb its spread (World Health Organization, 2020). These measures disrupted the services and treatments available to individuals battling opioid use addiction. For instance, clinics providing methadone and other addiction treatment medications were forced to close, and access to addiction support groups became limited (Rossen et al., 2020). The United States Drug Enforcement Administration allowed providers who were registered to prescribe schedule II-V controlled substances without requiring an in-person patient visit, but only through a telehealth visit (Rajagopal et al., 2023). Nationally, from 2019 to 2021, the total number of opioid-involved overdose deaths increased by 69% (National Institute of Health, US Department of Health and Human Services, 2023). In Georgia, this increase was even more pronounced, with a 101% rise in opioid-involved overdose deaths during the same period (Georgia Department of Public Health (GADPH), 2023). The direct and indirect impact of COVID-19 on opioid-related mortality is unknown due to data incompleteness, lack of coverage, and geographical disparities. These disparities have resulted in unreported deaths, potential misclassification of causes of death, and delayed death reports (Stokes et al., 2023).

Excess mortality has been used to assess the total impact of a crisis on public health outcomes

when direct information is either sparse or unavailable, and accuracy is questionable. Excess mortality is defined as the difference between observed death counts for a given time period and the expected number of deaths based on historical time trends pre-crisis (Rossen et al., 2020; Woolf et al., 2020; Mathieu et al., 2020; Wang et al., 2022; Msemburi et al., 2023; Blangiardo et al., 2020). Previous studies have assessed excess all-cause mortality due to COVID-19 at the national or sub-national levels. Woolf et al. (2020) examined state-specific levels of excess death from COVID-19 and other causes in the U.S. during the period March-July 2020 applying a Poisson regression model to obtain predicted expected deaths (Woolf et al., 2020). Rossen et al. (2020) published excess deaths associated with COVID-19 by age, race, and ethnicity for the U.S. during the period January 26-October 3, 2020 (Rossen et al., 2020). Blangiardo et al. (2020) estimated weekly spatio-temporal differences in excess mortality at the sub-national level in Italy from January 1- April 28 2020 applying a spatio-temporal disease mapping approach to evaluate excess mortality at the (small area) municipality level, while detecting and predicting its evolution on a weekly basis (Blangiardo et al., 2020). However, assessment of excess all-cause mortality at national and sub-national levels does not give a comprehensive understanding of the impact of COVID-19 on opioid users. Additionally, national and sub-national excess mortality estimates in the United States do not provide granular information on spatial-temporal variations within states and across counties. We extend the previously described methods to measure excess opioid mortality at the small area (county) level.

Our proposed Bayesian hierarchical excess opioid mortality (BHEOM) approach produces model-based estimates of the expected number of opioid overdoses based on previous observed spatial-temporal trends pre-pandemic, which is crucial for evaluating excess opioid mortality rates (Rossen et al., 2020; Sumetksy, N. et al., 2021; Wang et al., 2022). The model framework employs a spatio-temporal disease mapping approach, which is commonly used to investigate geographical-temporal variations of opioid mortality burden (Kline, D. et al., 2021; Hepler, S. et al., 2021). The standard Bayesian disease mapping model provides the capability to borrow strength and share information

across small areas thereby reducing high degrees of uncertainty associated with smaller population sizes (Waller, L.A. and Gotway, C.A., 2004; Wakefield, J., 2007). This is accomplished through spatial and temporal autocorrelation terms included within the hierarchical structure informing estimates of the unknown true risk of opioid-related death for a given county-time. Within our model framework, monthly opioid-related death counts between the years 2018-2019 are used to forecast county-month specific opioid mortality relative risk (RR) estimates for the years 2018-2020. The forecasted estimates capture the expected 2020 county-month specific opioid mortality trends in the absence of COVID-19. We derive estimates of excess mortality for 159 counties in Georgia by comparing the observed monthly number of opioid-related deaths to corresponding forecasted estimates representing the total impact of COVID-19 on opioid mortality rates. We illustrate model results for selected counties in Georgia to examine differing excess mortality trends across a wide variety of population sizes, and county characteristics. Using these findings, we aim to identify areas of greater need that require more intervention procedures, policies, and resource allocation to effectively address substance abuse, and counties suffering higher negative impact as a result of COVID-19.

This paper is organized as follows: Section 2.1 describes the data used to obtain excess opioid mortality estimates. Section 2.3 describes the data model assumed for the observed opioid death counts. Section 2.4 describes model assumption of the underlying process. Section 2.5 summarizes the process to obtain excess opioid mortality estimates and associated uncertainties. Lastly, Section 4 illustrates results across small, medium, and large population cases.

2. Methods

2.1. Data

Georgia Department of Public Health (GADPH) provided monthly opioid-related age-stratified death counts for all 159 counties in Georgia for the years 2018 through 2022 that were aggregated to county-month specific totals (Georgia Department of Public Health (GADPH), 2021). The

U.S. Census Bureau (USCB) publishes annual county-level population estimates using a cohort component model based on the last available census with adjustments for births, deaths, and net-migrations (U.S. Census Bureau, nd; Population Estimation Program, U.S. Census Bureau, 2019). Given the USCB does not report monthly population estimates, we assume that the population size remains constant throughout each respective year (12 months). Dividing the county-month specific opioid-related death total by the corresponding population estimate gives the crude rate of opioid overdoses by county-month from 2018-2022. Figure 1 illustrates the reported total count of opioid-related deaths across Georgia from 2018-2022. The red line signifies the onset of COVID-19 (Jan. 2020), and each respective color represents year-specific data. Figure 1 shows a relatively stable trend in reported total number of opioid-related deaths during pre-pandemic years. In 2020, the number of deaths increased with a significant spike in March. Between March 2020 and 2022, the number of deaths continues to rise over time, not reverting to pre-COVID-19 levels.

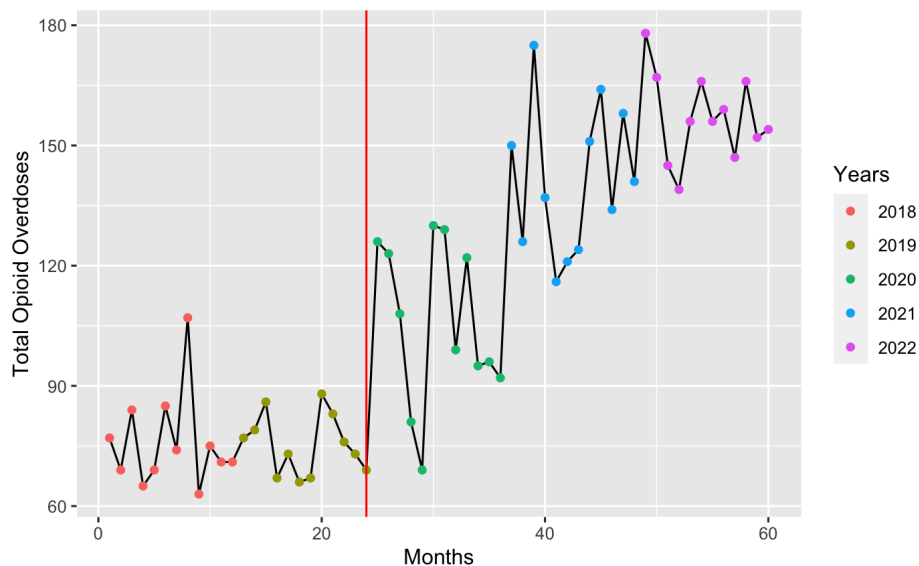


Figure 1: Monthly observed totals of opioid-related deaths across 159 counties in Georgia between the years 2018-2022. The red line denotes the defined start date of the COVID-19 pandemic (Jan. 2020). X-axis lists units in months ranging from 0 to 60, 0= Jan 2018, and 60 = Dec 2022. Colors denote years.

Figure 2 contains five maps of Georgia displaying the county-level crude rates of opioid related deaths (per 100,000 persons) by year. We note that higher rates occur in the years 2021 and 2022, a mass of higher rates is present mainly in the northwest region. The largest crude opioid

mortality rate pre-pandemic occurred in Taliaferro County (Population: 1,537 - 1,612) in 2019. It is worth mentioning that Taliaferro County, being the least populated county in Georgia, results in highly noisy rate estimates. The largest crude opioid mortality rate during COVID-19 occurred in Wilkinson County (Population: 8,824 - 9,043) in 2021. These exploratory findings motivate our model assumptions.

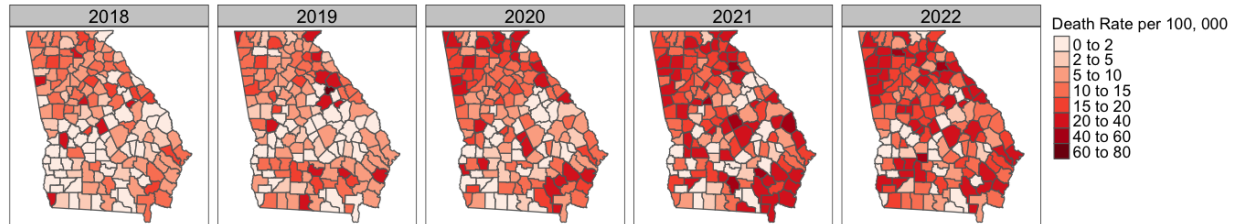


Figure 2: Mapped crude rates of opioid mortality (per 100,000) by year in Georgia between years 2018-2022. Color denotes the death rate per 100,000 which varies between 0 and 80.

2.2. Summary of model approach

Our Bayesian hierarchical excess opioid mortality (BHEOM) model estimates excess opioid mortality for 159 counties in Georgia to quantify the total (direct plus indirect) impact of COVID-19 on opioid mortality within the state. In our model approach we focus on estimating county-month specific opioid mortality rates, but note our approach could be applied to various spatial and temporal resolutions and socio-demographic sub-groups. The main features of the BHEOM model are as follows:

1. The *data model* (defining the likelihood function) consists of modeling observed county-month specific opioid-related death counts for 2018-2019 y_{im} using a Zero-Inflated Poisson assumption and is further detailed in Section 2.3.
2. The *process model* captures the latent true value of log-relative risk for county i month m denoted (θ_{im}) which is modeled as a function of spatial and temporal random effects defining the assumed underlying process. This is further described in Section 2.4.
3. Estimates of latent and true excess opioid mortality denoted χ_{im} are derived using posterior predictive distribution estimates of expected opioid overdose counts, further detailed in Section 2.5.

Appendix A illustrates a graphical representation of the BHEOM model set-up, refer to Appendix B for a summary of notation used.

2.3. Data model for observed opioid-mortality counts

In a standard disease mapping model, we commonly assume the relationship between the observed mortality counts and the true relative risk (i.e., the data model for observed cases) is given by a Poisson distribution which implicitly assumes cases in nearby areas are similar and the variance of response is equal to the mean not accounting for over-dispersion (Torabi, 2016). Given the nature of our observed mortality count data, which contains an excess of zero values, we model observed counts using a Zero-Inflated Poisson in Eq 1, which accounts for the over-dispersion caused by a mixture of data distributions (Agarwal et al., 2002; Ugarte et al., 2004; Rathbun and Fei, 2006; Wikle and Anderson, 2003). We denote observed counts for county i month m (labeled $[im]$ for ease of readability) as y_{im} . The contribution of the Poisson likelihood is determined by a mixing parameter π_{im} , representing the proportion of sample zeros. The county-month mixing parameter π_{im} is modeled hierarchically assuming a Bernoulli distribution with global parameter ρ truncated between 0 and 1. It is important to note here that, y_{im} is our given data, specifically data from years 2018 and 2019 excluding 2020-2022. The full data model is given by,

$$f(y_{im}|\theta_{im}, X_{im}) \sim \begin{cases} \pi_{im} + (1 - \pi_{im})e^{(X_{im}\theta_{im})} & \text{if } y_{im} = 0 \\ (1 - \pi_{im})\frac{\exp(-X_{im}\theta_{im})(X_{im}\theta_{im})^{y_{im}}}{y_{im}!} & \text{if } y_{im} > 0 \end{cases}, \quad \text{for } i = 1, \dots, 159, m = 1, \dots, 24 \quad (1)$$

$$\pi_{im} \sim \text{Bern}(\rho)$$

$$\rho \sim \text{Unif}(0, 1)$$

The expectation $E(y_{im}|\theta_{im}, X_{im}, \pi_{im})$, shown in Eq. 2, is written as a function of the expected count X_{im} , the log relative risk θ_{im} , and one minus the mixing parameter π_{im} . The offset X_{im} is equal to the product of the reference rate R and the population-at-risk N_{im} , which are both treated as fixed

and known. The reference rate is derived across populations and areas (from a much larger sample size) than are the local estimates, and so suffers from substantially less relative uncertainty.

$$\begin{aligned}
 E(y_{im}|\theta_{im}, X_{im}) &= \mu_{im} = (1 - \pi_{im})X_{im}\theta_{im} \\
 \text{Var}(y_{im}|\theta_{im}, X_{im}) &= \mu_{im} + \frac{\pi_{im}}{1 - \pi_{im}}\mu_{im}^2 \\
 X_{im} &= R \cdot N_{im} \\
 R &= \frac{\sum_{im} y_{im}}{\sum_{im} N_{im}}
 \end{aligned} \tag{2}$$

2.4. Process model for unobserved latent opioid mortality log-relative-risks

We model the latent log relative risk θ_{im} incorporating both spatially and temporally structured and unstructured random effects shown in Eq. 3. To incorporate spatial terms in our model, we consider the Besag-York-Mollie (BYM) Model (Riebler et al., 2016; Besag, J. et al., 1991; Knorr-Held, L., 2000; Waller, L.A. et al., 1997; Cressie, N. and Wikle, C.K., 2011), which allows us to estimate the relative risk of death weighting trends in the neighboring counties. We denote v_i to represent a spatially unstructured random effect term that is independent, identically, and normally distributed centered around zero, i.e., $v_i \sim N(0, \sigma_v^2)$. The spatially structured term, denoted u_i is modeled assuming an Intrinsic Conditional Auto-Regressive (ICAR) prior, which assumes complete correlation between neighboring areas. The spatial covariance matrix, W is written as a function of an $N \times N$ adjacency matrix where entries $\{i, i\}$ are zero and the off-diagonal elements are 1 if counties i and j are neighbors and 0 otherwise. D is the $N \times N$ diagonal matrix where entries $\{i, i\}$ are the number of neighbors of county i and the off-diagonal entries are 0. Lastly, τ denotes the smoothing parameter. It is important to note that our spatial parameters do not change over time. Let γ_m denote the time unstructured random effect term that is independent, identically, and normally distributed centered around zero, i.e., $\gamma_m \sim N(0, \sigma_\gamma^2)$. Correlated time trends are captured using a time structured random effect κ_m modeled with a random walk order 1 which assumes a constant trend in forecasted estimates. To capture the non-separable process of space-time, we introduce ω_{im} which captures the interaction between terms u and κ . As such

the interaction term captures the deviations away from the separable space-time trend (Rue, H. and Held, L., 2005). We model the interaction term as a first order random-walk within county. Using the complete process model, we obtain estimates of county-month specific log-transformed relative risks for years 2018-2020 including months without data, i.e., 2020.

$$\log(\theta_{im}) = \alpha + u_i + v_i + \kappa_m + \gamma_m + \omega_{im}, \quad \text{for } i = 1, \dots, 159, \quad m = 1, \dots, 36 \quad (3)$$

| | |
|---|---|
| $\alpha \sim N(0, \sigma_\alpha^2)$ | Intercept |
| $v_i \sim N(0, \sigma_v^2)$ | Unstructured Spatial Noise |
| $\mathbf{u} \sim N(0, [\tau(D - W)]^{-1})$ | (ICAR) prior for spatial auto-correlation |
| $\gamma_m \sim N(0, \sigma_\gamma^2)$ | Unstructured Temporal Noise |
| $\kappa_m \sim N(\kappa_{m-1}, \sigma_\kappa^2)$ | Random Walk(1) for temporal autocorrelation |
| $\omega_{im} \sim N(\omega_{i,m-1}, \sigma_\omega^2)$ | Random Walk(1) for space-time interaction |

2.5. Derivation of Excess mortality and associated uncertainties

To derive excess mortality estimates, we use the posterior predictive distribution (PPD) to obtain predicted counts of opioid related death for each county-month (Konstantinoudis et al., 2023). The PPD is represented by Eq. 4, where $p(\tilde{y}|y)$ represents the posterior distribution of expected counts \tilde{y} given the observed data y , and the posterior estimates of the log-relative risk $p(\theta_{im}|y_{im})$.

$$p(\tilde{y}|y) = \int_{\theta} p(\tilde{y}_{im}|\theta_{im}, y_{im}) p(\theta_{im}|y_{im}) d\theta_{im} \quad (4)$$

Using posterior predictive sample estimates of opioid death counts, denoted $\tilde{y}^{(s)}$ for samples $s = 1, \dots, S$, excess mortality sample estimates $\chi_{im}^{(s)}$ are equal to the difference between the observed and predicted values shown in Eq. 5. Median and 95% uncertainty intervals are calculated by taking the median, and 95% quantile estimates of the sample values $\chi_{im}^{(s)}$ across all S samples.

$$\chi_{im}^{(s)} = \tilde{y}_{im}^{(s)} - y_{im} \text{ for } m = 1, \dots, 36 \quad (5)$$

3. Computation

We extract PEP reported population estimates for 159 counties in Georgia, years 2018-2022, using the *tidycensus* package (Walker, K., 2020). For model processing and output, a Markov Chain Monte Carlo (MCMC) algorithm samples from the posterior distribution of the parameters via the software *Nimble* (de Valpine et al., 2017). Five parallel chains were run with a total of 3,000 iterations in each chain. Of these, the first 1,000 iterations in each chain are discarded so the resulting chains contain 2,000 samples. Additionally, we thinned the samples to retain every 10th iteration after burn-in. Thus for each parameters there was a total 1,000 saved posterior samples. Standard diagnostic checks using traceplots were used to check convergence (Plummer, 2017; Gelman and Rubin, 1992; Vehtari, A. et al., 2021; Su and Yajima, 2020; Rue, H. and Held, L., 2005; de Valpine et al., 2017).

4. Results

4.1. Global Parameter Estimates

Global and hyper parameters consist of the global variance terms σ_0^2 and the global level α . Table 1 shows posterior model-estimates and credible intervals for the global and hyper parameters.

| Parameters | Median | 95% CI Lower Bound | 95% CI Upper Bound |
|-------------------|--------|--------------------|--------------------|
| α | -0.223 | -0.515 | -0.034 |
| σ_α^2 | -0.264 | -1.092 | 0.579 |
| σ_κ^2 | 0.026 | 0.002 | 0.096 |
| σ_ν^2 | 0.153 | 0.071 | 0.32 |
| σ_γ^2 | 0.049 | 0.001 | 0.133 |
| σ_ω^2 | 0.165 | 0.098 | 0.226 |

Table 1: Global and hyper parameters included in the random effect terms of the (BHEOM) model.

4.2. Excess Across Georgia

Figure 3 illustrates total counts of predicted (green), observed (red), and excess (blue) opioid-related deaths across all of Georgia from 2018-2020. As noted in Figure 3, there is a stationary trend in the total number of deaths before the start of the pandemic in 2020. Our predicted monthly totals of deaths (green) wavered around 75 for all three years. In January 2020, the total count of observed (red) and excess (blue) began to rise, peaking in July 2020 with a total of 130 opioid-related deaths and an excess of 55 deaths. Excess mortality trends mimic the observed trends due to relatively stationary model-based predictive estimates indicating that the pandemic resulted in a stark increase in excess opioid mortality deaths across the entire state of Georgia.

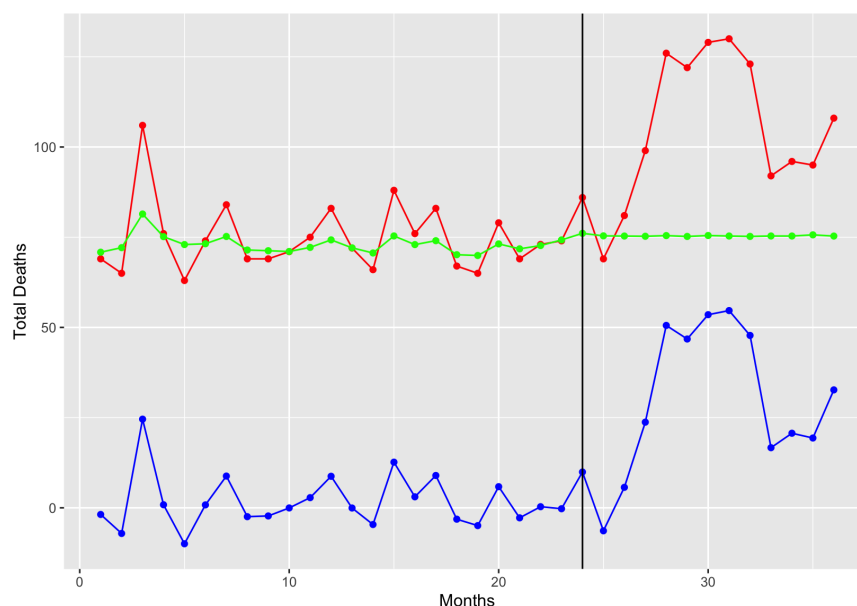


Figure 3: Monthly totals of predicted, observed, and excess opioid-related deaths across 159 counties in Georgia between the years 2018-2020. The black line denotes the defined start of the COVID-19 pandemic in the model. The X-axis lists units in months ranging from 0 to 36, 0 = Jan 2018, and 36 = Dec 2020. Line colors distinguish the data source, red = observed deaths, lime green = predicted deaths, and blue = excess deaths.

Figure 4 contains three maps of Georgia displaying the median excess rates of opioid mortality (per 100,000) per respective county by year. In comparison to the map of Georgia for 2018, the map of Georgia for 2020 illustrates that many counties experienced an increase in excess death rates after the start of COVID-19 after controlling for population size. In 2020, McIntosh County (Population: 10,987 - 14,378) experienced the highest median excess rate of 8.44 (7.69, 8.79) and

Franklin County (Population: 23,034 - 23,468) experienced the lowest median excess rate of -1.26 (-2.23, -0.72). It is important to note that negative excess death rates occur when the observed opioid mortality count is lower than the predicted opioid mortality count.

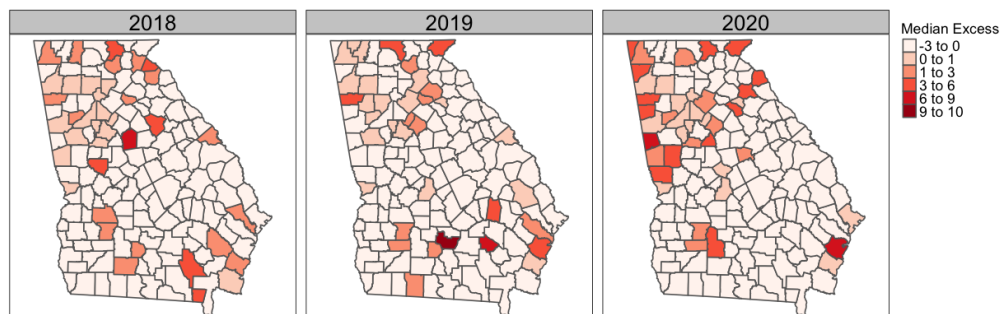


Figure 4: Mapped excess rates of opioid mortality (per 100,000) by year in Georgia between years 2018-2020. Colors distinguish the rates and the rates vary between 0 and 9.

4.3. Large County Population Cases

Figure 5 illustrates excess opioid mortality trends for selected largely populated counties within Georgia including DeKalb, Fulton, and Gwinnett County. Each respective county plot represents the predicted (green), observed (red), and excess (blue) rates of opioid mortality rate (per 100,000) by month for years 2018-2020.

In DeKalb County (Population: 754,906 - 764,420), the observed monthly opioid-related death rates range between 0 and 1.5 for 2018-2020. Its predicted monthly opioid-related death rate is stationary around 0.66. DeKalb County experienced its highest excess death rate of 0.79 (0.62, 0.92) in May 2020 and its lowest excess death rate of -0.66 (-0.81, -0.53) in February 2018.

In Fulton County (Population: 1,050,131 - 1,069,370), the observed monthly opioid-related death rates occur between 0.1 and 2.0 for 2018-2020. Its predicted monthly opioid-related death rate is consistently around 0.72. Fulton County experienced its highest excess death rate of 0.97 (0.81, 1.12) in May 2020 and its lowest excess death rate of -0.51 (-0.65, 0.39) in July 2019.

In Gwinnett County (Population: 927,337 - 958,005), the observed monthly opioid-related death rates range between 0 and 2.0 for 2018–2020. Its predicted monthly opioid-related death rate is centered around 0.6 for all three years. Gwinnett County experienced its highest excess death rate of 1.07 (0.9, 1.19) in December 2020 and its lowest excess death rate of 0.6 (-0.72, 0.49) in May 2018.

Comparing excess mortality rates across the selected counties illustrates that all counties shown below experienced a peak of excess mortality after the start of the pandemic. Furthermore, the plots show that uncertainty surrounding model-based estimates increases during the pandemic months when data has been removed. Consequently, forecast estimates experience higher levels of uncertainty.

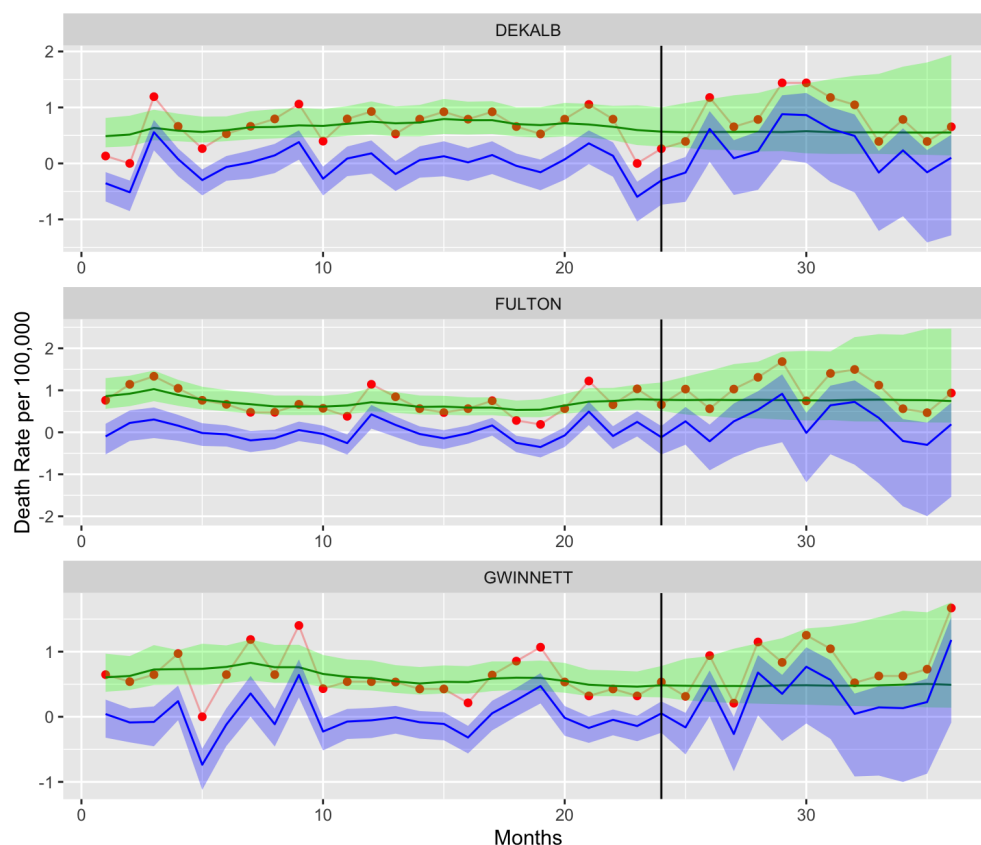


Figure 5: Monthly predicted, observed, and excess (and associated 95% confidence intervals) rates of opioid mortality (per 100,000) across DeKalb, Fulton, and Gwinnett County. The black line denotes the defined start of the COVID-19 pandemic in the model. The X-axis lists units in months ranging from 0 to 36, 0 = Jan 2018, and 36 = Dec 2020. Line colors distinguish the data source, red = observed deaths, lime green = predicted deaths, and blue = excess deaths.

4.4. Moderate County Population Cases

Figure 6 illustrates selected cases of moderate (medium) populated counties within Georgia including Bartow, Cherokee, and Clayton County.

In Bartow County (Population: 106,378 - 109,296), the observed monthly opioid-related death rates range between 0 and 6 for 2018–2020. The predicted monthly opioid-related death rate is centered around 1.3. Bartow County experienced its highest excess death rate of 4.29 (3.79, 4.62) in May 2020 and its lowest excess death rate of 1.2 (-1.72, -0.86) in April 2018.

In Cherokee County (Population: 253,914 - 268,175), the observed monthly opioid-related death rates range between 0 and 4 for 2018–2020. Its predicted monthly opioid-related death rate is consistently around 0.9. Cherokee County experienced its highest excess death rate of 2.96 (2.66, 3.19) in March 2018 and its lowest excess death rate of -0.95 (-1.24, 0.72) in January 2020.

In Clayton County (Population: 289,197 - 297,623), the observed monthly opioid-related death rates range between 0 and 2 for 2018–2020. Its predicted monthly opioid-related death rate maintains around 0.4. Clayton County experienced its highest excess death rate of 1.57 (1.4, 1.71) in June 2020 and its lowest excess death rate of -0.45 (-0.62, -0.31) in February 2018.

For all three counties, the excess mortality rates increased after the onset of COVID-19 indicating a similar pattern shown in the larger counties in Figure 5. However, it is important to also note, that small to moderate counties also suffer from increased levels of variability in both observed and predicted estimates due to smaller population sizes. The excessively high increase in opioid death rate for Cherokee County (March 2018) does not follow the trend of observed counts, which illustrates large changes in death rates occur with slight increases in death counts for medium/smaller counties. The plots illustrate the benefit of the BBHEOM approach which allows for sharing of information across counties to reduce uncertainty in estimates for smaller and moderate counties

and imposes a degree of smoothing of erratic rates.

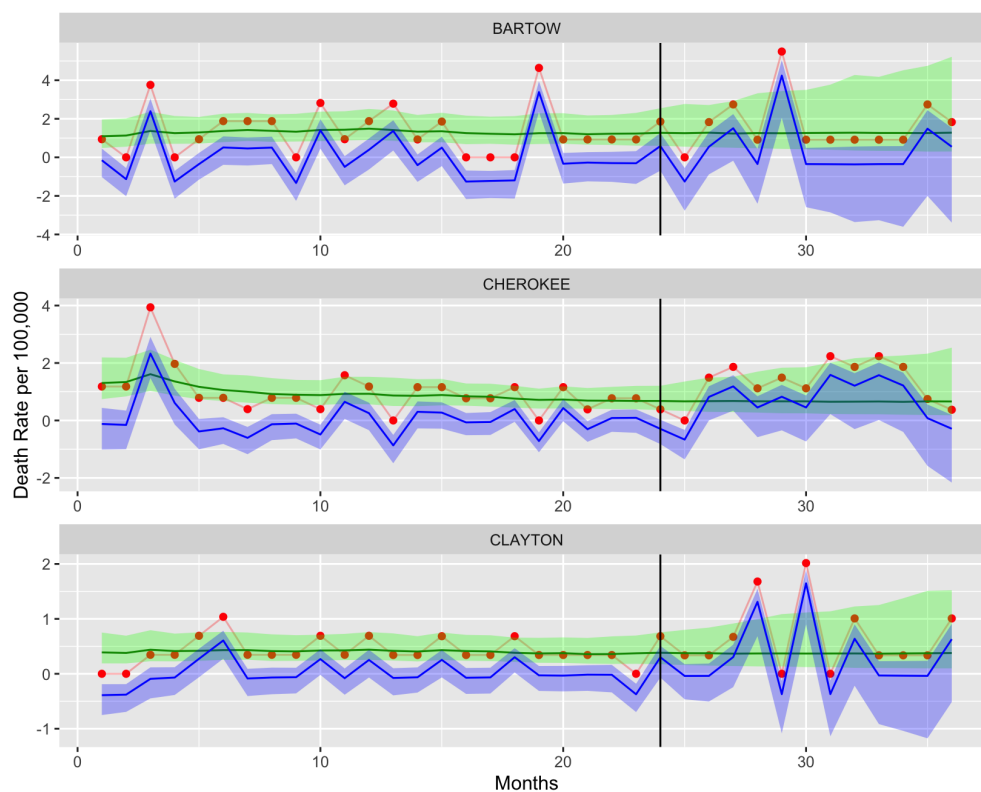


Figure 6: Monthly predicted, observed, and excess (and associated 95% confidence intervals) rates of opioid mortality (per 100,000) across Bartow, Cherokee, and Clayton County. The black line denotes the defined start of the COVID-19 pandemic in the model. The X-axis lists units in months ranging from 0 to 36, 0 = Jan 2018, and 36 = Dec 2020. Line colors distinguish the data source, red = observed death rates, lime green = predicted death rates, and blue = excess death rates.

4.5. Small County Population Cases

Figure 7 contains selected cases of small populated counties within Georgia including Toombs, Meriwether, and Walker County.

In Toombs County (Population: 26,830 - 27,081), the observed monthly opioid-related death rates range between 0 and 5 for 2018–2020. Its predicted monthly opioid-related death rate maintains around 0.44. Toombs County experienced its highest excess death rate of 3.28 (2.85, 3.52) in December 2019 and its lowest excess death rate of -0.46 (-0.88, -0.22) in March 2018.

In Meriwether County (Population: 20,606 - 21,167), the observed monthly opioid-related death rates range between 0 and 10 for 2018 – 2020. Its predicted monthly opioid-related death rate maintains around 0.64. Meriwether County experienced its highest excess death rate of 8.84 (8.27, 9.17) in April 2018 and its lowest excess death rate of -0.66 (-1.26, -0.32) in March 2018.

In Walker County (Population: 67,742 - 69,761), the observed monthly opioid-related death rates range between 0 and 3 for 2018–2020. Its predicted monthly opioid-related death rate maintains around 0.85. Walker County experienced its highest excess death rate of 2.11 (1.67, 2.41) in November 2020 and its lowest excess death rate of -0.86 (-1.29, -0.56) in April 2018.

Figure 7 illustrates the stark and rapid changes in observed death rates that often occur due to singular deaths during particular times. Additionally, in these smaller counties, there are zero deaths for the majority of months. As such, excess mortality estimates obtained from the BHEOM model capture the negative excess mortality rates in periods where there are zero deaths, and the increase in excess mortality in months where there are deaths present.

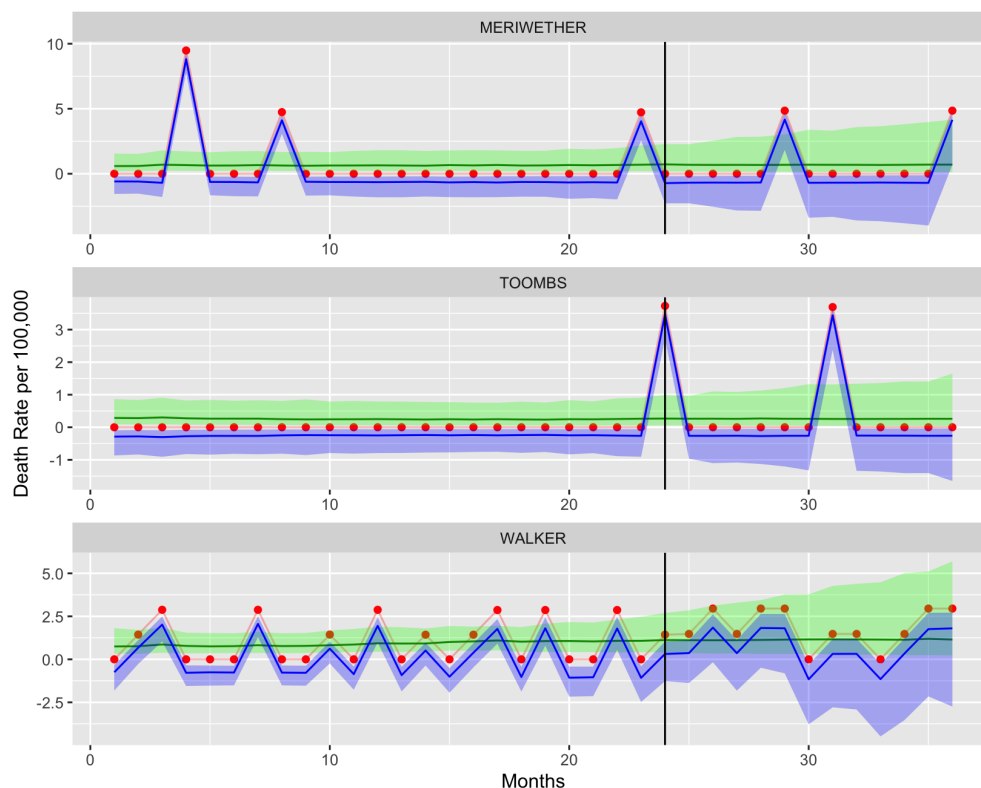


Figure 7: Monthly predicted (and associated 95% confidence intervals), observed, and excess (and associated 95% confidence intervals) rates of opioid mortality (per 100,000) across Toombs, Meriwether, and Walker County. The black line denotes the defined start of the COVID-19 pandemic in the model. The X-axis lists units in months ranging from 0 to 36, 0 = Jan 2018, and 36 = Dec 2020. Line colors distinguish the data source, red = observed death rates, lime green = predicted death rates, and blue = excess death rates.

5. Discussion

Evaluating the impact of COVID-19 on opioid drug use is difficult due to the lack of real time cause-specific death data and inaccurate record keeping of COVID-19 cases. To address this, we have presented a Bayesian hierarchical excess opioid mortality model in which: (1) explores the spatio-temporal variations in opioid deaths for 159 counties in Georgia, and (2) assesses excess opioid mortality pre- and post- the COVID-19 pandemic. The general findings suggest that COVID-19 did act as a catalyst in excess opioid mortality. Pre-COVID-19, Georgia's monthly excess opioid related deaths did not exceed fifty. Post-COVID-19, Georgia's monthly excess opioid related deaths have spiked over fifty and forecasts to continue to increase. The county population size cases display key features of our model's performance and reactions to death counts, which

vary based on the county's population size. In large counties, findings showed that they experienced an increase in their excess death rates post-COVID-19. In moderate size counties, larger variability is observed in their excess death rates due to the impact of deaths on their smaller population size. In smaller counties, the erratic nature of opioid mortality deaths illustrated the stark change in death rates due to a small number of individual events. Our findings guide understanding of the total impact of COVID-19 on opioid users within each county.

The contributions of this work to statistical modeling and excess opioid mortality are two-fold. Firstly, we expanded upon existing work that was done to evaluate excess mortality geographically as a result of COVID-19 to produce model-based excess mortality estimates at granular levels. Secondly, our developed methodology can be applied to assist in small area excess mortality estimation in other applications including other epidemics/pandemics, natural disasters, law regulations, mental health disorders, and more.

We also note the limitations of our study. Firstly, we observed a high number of zero values, which resulted in stationary estimates over time. In an attempt to address this issue, we replaced the use of a Poisson distribution in the standard disease mapping approach with a Zero-Inflated Poisson distribution. Secondly, in general, there is variability in forecasting and predicting time trends based on limited data. Improving upon this limitation requires Georgia to address its record keeping and procedures of deaths, specifically overdose related deaths and COVID-19 deaths.

In our future analyses, we plan to incorporate informative and predictive factors that may aid in the estimation and forecasting of opioid mortality trends, i.e., social determinants of health. In the future, our results could play a pivotal role in shaping public health policies related to opioid use and assessing resource allocations and disaster response to counties in Georgia in need of support in addressing substance abuse.

Bibliography

Wakefield, J., Disease mapping and spatial regression with count data, *Biostatistics* 8 (2007) 158–183. doi:10.1093/biostatistics/kx1008.

World Health Organization, Who director-general's opening remarks at the media briefing on covid-19 - 11 march 2020., www.who.int/director-general/speeches/detail/who-director-general-s-opening-remarks-at-the-media-briefing-on-covid-19---11-march-2020, 2020.

L. M. Rossen, A. M. Branum, F. B. Ahmad, P. Sutton, R. N. Anderson, Excess deaths associated with covid-19, by age and race and ethnicity—united states, january 26–october 3, 2020, *Morbidity and Mortality Weekly Report* 69 (2020) 1522.

S. Rajagopal, J. Westra, M. A. Raji, D. Wilkes, Y.-F. Kuo, Access to medications for opioid use disorder during covid-19: Retrospective study of commercially insured patients from 2019–2022, *American Journal of Preventive Medicine* (2023).

National Institute of Health, US Department of Health and Human Services, Drug overdose death rates, www.nida.nih.gov/research-topics/trends-statistics/overdose-death-rates, 2023. Accessed on 06-30-2023.

Georgia Department of Public Health (GADPH), General overview, www.dph.georgia.gov/stopopioidaddiction, 2023. URL: www.dph.georgia.gov/stopopioidaddiction, accessed on 02-01-2023.

A. Stokes, D. Lundberg, E. Wrigley-Field, Y.-H. Chen, Covid-19 deaths in the us continue to be undercounted, despite claims of "overcounts", 2023. URL: www.bu.edu/sph/news/articles/2023/covid-19-deaths-in-the-us-continue-to-be-undercounted-research-shows-despite-claims-of-overcounts/.

S. H. Woolf, D. A. Chapman, R. T. Sabo, D. M. Weinberger, L. Hill, D. D. Taylor, Excess deaths from covid-19 and other causes, march-july 2020, *Jama* 324 (2020) 1562–1564.

- E. Mathieu, H. Ritchie, L. Rodés-Guirao, C. Appel, C. Giattino, J. Hasell, B. Macdonald, S. Dattani, D. Beltekian, E. Ortiz-Ospina, et al., Coronavirus pandemic (covid-19), Our world in data (2020).
- H. Wang, K. R. Paulson, S. A. Pease, S. Watson, H. Comfort, P. Zheng, A. Y. Aravkin, C. Bisignano, R. M. Barber, T. Alam, et al., Estimating excess mortality due to the covid-19 pandemic: a systematic analysis of covid-19-related mortality, 2020–21, *The Lancet* 399 (2022) 1513–1536.
- W. Msemburi, A. Karlinsky, V. Knutson, S. Aleshin-Guendel, S. Chatterji, J. Wakefield, The who estimates of excess mortality associated with the covid-19 pandemic, *Nature* 613 (2023) 130–137.
- M. Blangiardo, M. Cameletti, M. Pirani, G. Corsetti, M. Battaglini, G. Baio, Estimating weekly excess mortality at sub-national level in italy during the covid-19 pandemic, *PLOS ONE* 15 (2020) 1–15. URL: <https://doi.org/10.1371/journal.pone.0240286>. doi:10.1371/journal.pone.0240286.
- Sumetksy, N., Mair, C., Wheeler-Martin, K., Magdalena, C., Waller, L.A., Ponicki, W.R., Grunewald, P.J., Predicting the future course of opioid overdose mortality: An example from two us states, *Epidemiology* 32 (2021) 61–69.
- Kline, D., Pan, Y., Hepler, S., Spatio-temporal trends in opioid overdose deaths by race for counties in ohio, *Epidemiology* 32 (2021) 295–302.
- Hepler, S., Waller, L.A., Kline, D.M., A multivariate spatiotemporal change-point model of opioid overdose deaths in ohio, *Annals of Applied Statistics* 15 (2021) 1329–1342.
- Waller, L.A., Gotway, C.A., *Applied Spatial Statistics for Public Health Data*, John Wiley & Sons, Inc., 2004. doi:10.1002/0471662682.
- Georgia Department of Public Health (GADPH), Drug surveillance unit: Drug overdose-mortality

web query, <https://www2.census.gov/programs-surveys/popest/technical-documentation/methodology/2010-2019/natstcopr-methv2.pdf>, 2021. Accessed on 09-01-2022.

U.S. Census Bureau, Explore census data, n.d. URL: <https://data.census.gov/>.

Population Estimation Program, U.S. Census Bureau, Methodology for the united states population estimates: Vintage 2019 (2019). URL: <https://www2.census.gov/programs-surveys/popest/technical-documentation/methodology/2010-2019/natstcopr-methv2.pdf>, accessed on 07-05-2021.

M. Torabi, Hierarchical multivariate mixture generalized linear models for the analysis of spatial data: An application to disease mapping), *Biometrical Journal* (2016).

C. Agarwal, G. Green, M. Grove, T. Evans, C. Schweik, A Review and Assessment of Land-Use Change Models. *Dynamics of Space, Time, and Human Choice*, 2002.

M. Ugarte, B. Beroiz, A. Militino, Testing for poisson zero inflation in disease mapping, *Biometrical Journal* 46 (2004) 526 – 539. doi:10.1002/bimj.200310061.

S. Rathbun, S. Fei, A spatial zero-inflated poisson regression model for oak regeneration, *Environmental and Ecological Statistics* 13 (2006) 409–426. doi:10.1007/s10651-006-0020-x.

C. K. Wikle, C. J. Anderson, Climatological analysis of tornado report counts using a hierarchical bayesian spatiotemporal model, *Journal of Geophysical Research: Atmospheres* 108 (2003). doi:<https://doi.org/10.1029/2002JD002806>.

A. Riebler, S. H. Sørbye, D. Simpson, H. Rue, An intuitive bayesian spatial model for disease mapping that accounts for scaling, *Statistical methods in medical research* 25 (2016) 1145–1165.

Besag, J., York, J., Mollie, A., Bayesian image restoration with two applications in spatial statistics (with discussion), *Annals of the Institute of Statistical Mathematics* 43 (1991) 1—59.

Knorr-Held, L., Bayesian modelling of inseparable space-time variation in disease risk, *Statistics in Medicine* 19 (2000) 2555–2567.

Waller, L.A., Carlin, B.P., Xia, H, Gelfand, A.E, Hierarchical spatio-temporal mapping of disease rates, *Journal of the American Statistical Association* 92 (1997) 607–617.

Cressie, N.and Wikle, C.K., *Statistics for Spatio-Temporal Data*, first ed., Wiley & Sons, 2011.

Rue, H., Held, L., *Gaussian Markov Random Fields*, Chapman & Hall/CRC, 2005.

G. Konstantinoudis, V. Gómez-Rubio, M. Cameletti, M. Pirani, G. Baio, M. Blangiardo, A workflow for estimating and visualising excess mortality during the covid-19 pandemic, *The R Journal* 15 (2023) 89–104.

Walker, K., tidycensus: Load us census boundary and attribute data as ‘tidyverse’. r package version 0.9.9.2, <https://walker-data.com/tidycensus/articles/basic-usage.html>, 2020. URL: <https://walker-data.com/tidycensus/articles/basic-usage.html>, accessed: 08-10-2022.

P. de Valpine, D. Turek, C. Paciorek, C. Anderson-Bergman, D. Temple Lang, R. Bodik, Programming with models: writing statistical algorithms for general model structures with NIMBLE, *Journal of Computational and Graphical Statistics* 26 (2017) 403–413. doi:10.1080/10618600.2016.1172487.

M. Plummer, *JAGS: A program for analysis of Bayesian graphical models using Gibbs sampling* (2017).

A. Gelman, D. B. Rubin, Inference from Iterative Simulation Using Multiple Sequences, *Statistical Science* 7 (1992) 457–472. URL: <http://www.jstor.org/stable/2246093>, publisher: Institute of Mathematical Statistics.

Vehtari, A., Gelman, A., Simpson, D., Carpenter, B., Bürkner, P.C., Rank-Normalization, Folding, and Localization: An Improved \widehat{R} for Assessing Convergence of MCMC (with

Discussion), *Bayesian Analysis* 16 (2021) 667–718. URL: <https://doi.org/10.1214/20-BA1221>.
doi:10.1214/20-BA1221.

Y.-S. Su, M. Yajima, *R2jags: Using R to Run 'JAGS'*, <https://CRAN.R-project.org/package=R2jags>, 2020. URL: <https://CRAN.R-project.org/package=R2jags>, accessed 2020-07-09.

Appendix A. Graphical representation of the BHEOM model

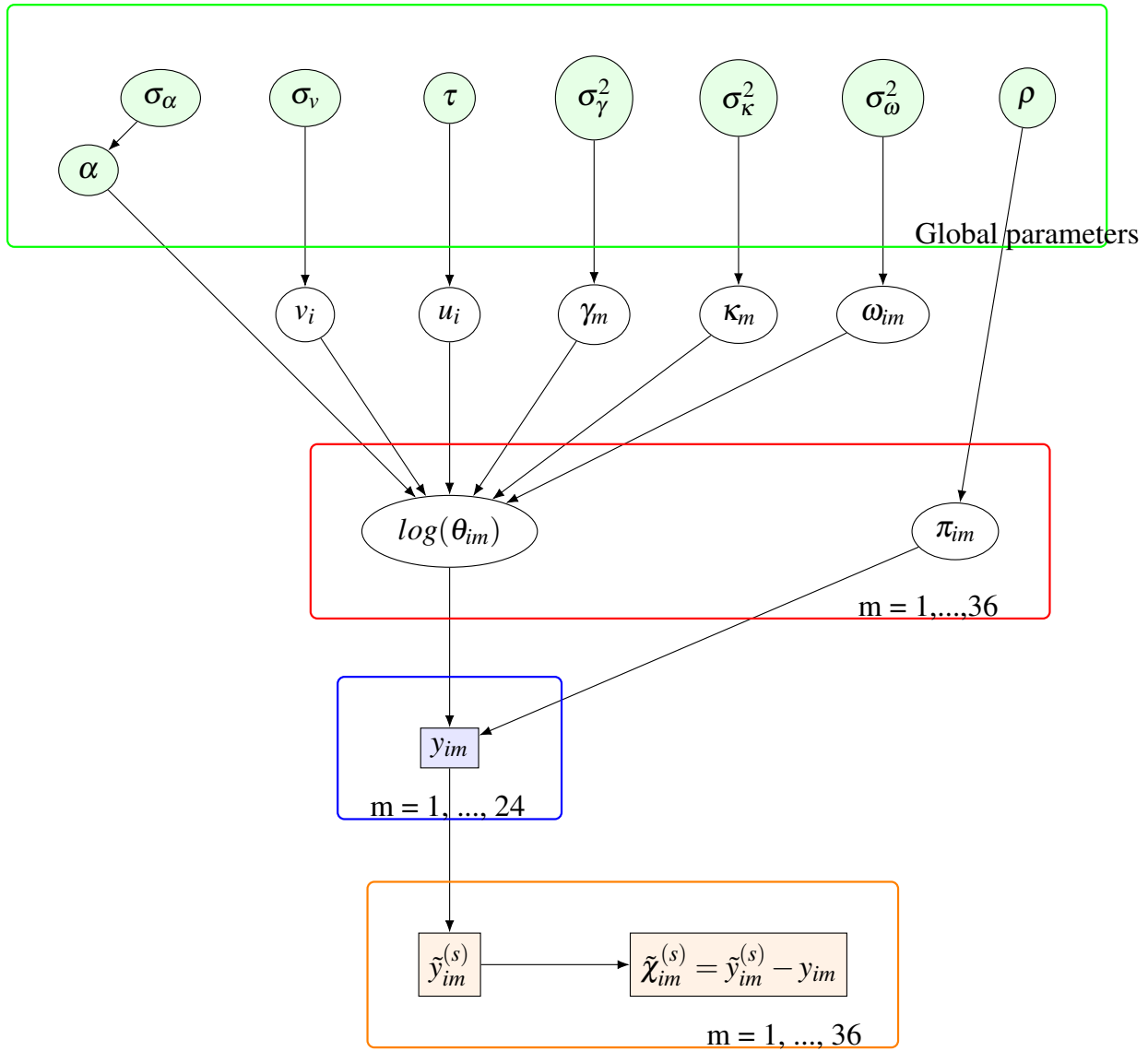


Figure A.8: Directed graphical representation of the BHEOM hierarchical model. Shaded rectangles denote observed data quantities, and circles denote latent variables (shaded circles for global hyper-parameters). Solid arrows denote stochastic dependency. Boxes group quantities by indices, i.e., (1) Bottom box contains observed population data, stratified by county-month for years 2018-2019, (2) Middle box contains estimated parameters stratified by county-month, for years 2018-2020, (3) Top box contains global parameters. Subscripts refer to county i , month m .

Appendix B. Notation Table

| Parameter Notation | Description |
|-----------------------------|---|
| Data Quantities | |
| R | Reference risk |
| N_{im} | Population for county i , month m |
| y_{im} | Opioid mortality counts for county i , month m |
| θ_{im} | Log relative risk for county i , month m |
| X_{im} | Population at risk for county i , month m |
| π_{im} | Poisson likelihood mixing parameter for county i , month m |
| Estimates Quantities | |
| α | Overall Intercept |
| σ_{α}^2 | Variance of the intercept |
| v_i | Spatially unstructured random effect term |
| σ_v^2 | Variance of the spatially unstructured random effect |
| \mathbf{u} | Spatial auto-correlation (ICAR prior) |
| τ | Smoothing parameter of the ICAR prior |
| D | Diagonal matrix containing the number of neighbors of each area on the diagonal |
| W | Adjacency matrix containing 1 for neighboring & 0 for non-neighboring counties |
| γ_m | Temporal unstructured random effect term |
| σ_{γ}^2 | Variance of the temporal unstructured random effect |
| κ_m | Temporal autocorrelation (RW(1)) |
| σ_{κ}^2 | Variance of the temporal structured random effect |
| ω_{im} | Space-time interaction term (RW(1)) |
| σ_{ω}^2 | Variance of the interaction between temporal and spatial effects |